

# A Microscopic Energy- and Density-Dependent Effective Interaction and its Test by Nucleus-Nucleus Scattering <sup>1</sup>

G. Bartnitzky<sup>a</sup>, H. Clement<sup>a</sup>, P. Czerski<sup>b,c</sup>, H. Müther<sup>b</sup>, F. Nuoffer<sup>a</sup>, J. Siegler<sup>a</sup>

<sup>a</sup>Physikalisches Institut, Universität Tübingen, D-72076 Tübingen, Germany

<sup>b</sup>Institut für Theoretische Physik, Universität Tübingen,  
D-72076 Tübingen, Germany

<sup>c</sup>Institute of Nuclear Physics, 30152 Krakow, Poland

**Abstract:** An effective nucleon-nucleon interaction calculated in nuclear matter from the Bonn potential has been parametrized in terms of a local density- and energy-dependent two-body interaction. This allows to calculate the real part of the nucleus-nucleus scattering potential and to test this effective interaction over a wide region of densities ( $\rho \leq 3\rho_0$ ) produced dynamically in scattering experiments. Comparing our calculations with empirical potentials extracted from data on light and heavy ion scattering by model-unrestricted analysis methods, we find quantitative agreement with the exception of proton scattering. The failure in this case may be traced back to the properties of the effective interaction at low densities, for which the nuclear matter results are not reliable. The success of the interaction at high overlap densities confirms the empirical evidence for a soft equation of state for cold nuclear matter.

PACS: 21.30.+y, 21.65.+f, 25.40.Cm, 25.55.Ci, 25.70.Bc

Keywords: Effective Nucleon-Nucleon Interaction, Density Dependence, Nucleus-Nucleus Scattering, Nuclear Matter

The effective interaction between nucleons bound in a nuclear medium is of fundamental interest for the understanding of nuclear structure aspects as well as of astrophysical problems like neutron stars and super nova phenomena. For the latter the behavior of the effective interaction at high densities and low temperature is crucial. In the laboratory this region is only accessible dynamically in nucleus-nucleus scattering, where the real central scattering potential is strongly affected by the density dependence of the underlying effective nucleon-nucleon (NN) interaction. In the experiment sensitivity to the real central potential is obtained by the observation of refractive scattering phenomena. Since diffractive and absorptive processes dominate the scattering process in particular for heavy scattering systems, the observation of nuclear rainbow scattering is mandatory

---

<sup>1</sup>Supported by the DFG (Mu 705/3, Graduiertenkolleg) and contract F-39 11 FMSC-PAA/NSF-94-158 (Poland)

for a sufficient sensitivity to the real central potential in case of composite particle scattering. In such a case real and imaginary parts of the potential can be extracted reliably by model-unrestricted analysis methods from angular distributions measured with high precision [1-4].

Assuming a local NN-interaction the real scattering potential is obtained by convolution of this effective NN-interaction with the point nucleon densities of target and projectile. Antisymmetrisation in this double folding method is accounted for by the exchange potential, which we have calculated in the finite range approximation [5,6]. For the nucleon density distributions in projectile ( $\rho_P$ ) and target ( $\rho_T$ ) we have used the empirical results from electron scattering. In previous double folding calculations it has been common to factorize the effective NN interaction  $v$  for convenience into  $v(s, E, \rho) = g(s, E) \cdot f(\rho)$ , where  $s, E, \rho$  denote NN-distance, energy of the NN-pair and density of the surrounding medium, respectively. For  $g(s, E)$  usually a *M3Y*-type effective interaction [7], based on the Reid-Elliott or the Paris potential (and derived actually for a specific system,  $^{16}\text{O}$ , only), has been chosen. The energy dependence then originates exclusively from the treatment of the exchange potential. For  $f(\rho)$  a purely phenomenological ansatz has been made with parameters fitted to describe scattering data for light and heavy ions. In that kind of double folding analyses it has been shown [1-5,8] that at large overlap densities  $\rho > \rho_0$ , where  $\rho_0 = 0.17 \text{ fm}^{-3}$  is the saturation density of nuclear matter, the density dependence of  $v$  has to be weak in order to be compatible with scattering data, whereas for  $\rho < \rho_0$  the density dependence has to be quite strong [2]. Fig. 1 shows the results of such analyses for  $f(\rho)$  as obtained from fits to data for light ion [2,3] and heavy ion [4] scattering. The hatched areas give the uncertainties as estimated in these analyses. As may be seen, the main sensitivity of heavy ion scattering is for  $\rho \gtrsim \rho_0$ , whereas the behavior at low densities is fixed by light ion scattering, in particular by proton scattering [2]. We also note that for  $\rho \gtrsim \rho_0$  our findings are compatible within the plotted error bands to the results of Refs. [5,8] for alpha and heavy ion scattering.

In this paper we present a new, more basic approach, for which we no longer require that the density dependence of the effective NN-interaction factorizes and is adjusted purely phenomenologically. We rather derive  $v(s, E, \rho)$  without adjustment of any parameter from the *G*-matrix calculated in a nuclear matter approach from a realistic NN-interaction.

Starting point of our investigation is the *G*-matrix calculated by solving the Bethe-Goldstone equation in nuclear matter [9,10]

$$G(\rho, E) = V + V \frac{Q}{E - QTQ} G(\rho, E). \quad (1)$$

Our choice for the realistic NN potential  $V$  has been the One-Boson-Exchange potential  $B$  as defined in table A.1 of [9]. This potential is realistic in the sense that it has been fitted to describe the NN scattering data and the properties of

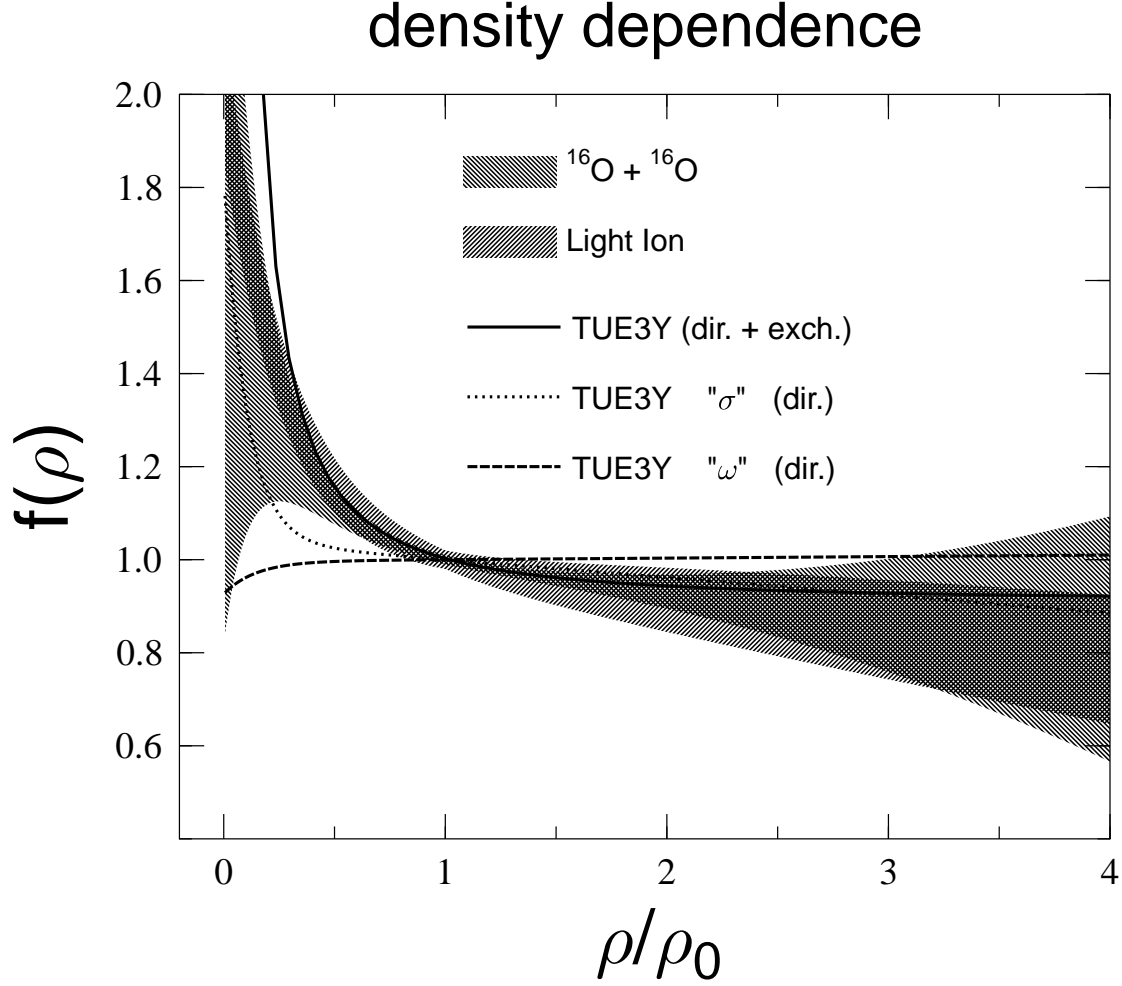


Figure 1: Density dependence  $f(\rho)$  of the effective NN-interaction in the factorized form  $v(s, E, \rho) = g(s, E)f(\rho)$ . The hatched areas give the result of double folding analyses of light and heavy ion scattering. The dash-dotted and dashed curves show the density dependence of “ $\sigma$ ” and “ $\omega$ ” exchange in the isoscalar-scalar part (direct term only) of our effective NN-interaction. The solid curve gives the density dependence of the full interaction (direct + exchange parts) for nuclear matter, i.e. without any nuclear surface effects.

the deuteron. The Bethe-Goldstone equation can be considered as an extension of the Lippman-Schwinger equation of the reaction matrix for NN scattering to a system of a density  $\rho$ . Therefore  $G$  describes the effective interaction of two nucleons in the medium, accounting for the effects of correlations. The Pauli operator  $Q$  in (1), with eigenvalues 0 for two-particle states with one of the nucleons occupying a state with momentum below the Fermi momentum and 1 else, prevents scattering into intermediate states which violate the Pauli principle. The Pauli operator is the source of the density dependence of  $G$ . Furthermore  $G$  depends on the starting energy,  $E$ , which is the energy of the interacting pair of nucleons. It is given by  $E = E_{\text{kin}}/A - \langle S_P \rangle - \langle S_T \rangle$ , where  $\langle S_P \rangle$  and  $\langle S_T \rangle$  are the average nucleon separation energies of projectile and target, respectively.  $T$  represents the operator for the kinetic energy and yields the energies of the intermediate particle states in the propagator of (1).

In a next step we want to parametrize the effective interaction  $G$  in terms of a local two-body interaction, keeping track of the density and energy dependence. For that purpose we consider an ansatz for the local interaction which is of the form

$$V_{\text{Local}} = f(q) + f'(q)\vec{\tau}_1 \cdot \vec{\tau}_2 + g(q)\vec{\sigma}_1 \cdot \vec{\sigma}_2 + g'(q)\vec{\sigma}_1 \cdot \vec{\sigma}_2 \vec{\tau}_1 \cdot \vec{\tau}_2, \quad (2)$$

where the function  $f(q)$  for the central scalar-isoscalar term is parameterized as a function of the momentum transfer  $q$  in terms of two Yukawa potentials

$$f(q) = \sum_{i=1}^2 \frac{A_i}{m_i^2 + q^2}. \quad (3)$$

The ranges of these two Yukawa potentials, defined by the “meson”-masses  $m_i$  have been chosen identical to the  $M3Y$  parametrization of [7], which means  $m_1 = 493.3$  MeV and  $m_2 = 789.28$  MeV representing the masses of the “ $\sigma$ ” and “ $\omega$ ” meson, respectively. A corresponding ansatz has also been made for the other functions ( $f'(q)$ ,  $g(q)$ ,  $g'(q)$ ) assuming the same values for the masses  $m_i$ . Only for the spin-isovector term ( $g'$ ) the pion ( $m_3 = 139.55$  MeV) has been considered explicitly, fixing the coupling constant to the value which has also been used for the  $M3Y$  parametrization. The parameters for the coupling constants ( $A_i$ , and corresponding ones for the other channels) have been adjusted such that the local interaction  $V_{\text{Local}}$  fits the antisymmetrized matrix elements calculated for the  $G$ -matrix at a given density  $\rho$  and starting energy  $E$ , i.e.  $A_i = A_i(\rho, E)$  etc. This means that at each energy and density, the  $G$ -matrix is parametrized in terms of 8 coupling constants. The required effective NN-interaction  $v(s, E, \rho)$  is then just given by the Fourier transformation of (2) and (3), respectively. As a result one finds that the energy- and momentum-dependence of  $A_i$  in general is rather weak. Strong deviations are only observed at small densities and large starting energies  $E$ . This special behavior of the parameters at small densities may be interpreted as an indication that the attempt to derive a local effective interaction from the  $G$ -matrix of nuclear matter at densities far below the saturation density does not

produce very reliable results. This may reflect the fact that the homogeneous nuclear matter at these densities is instable against the formation of droplets. Hence for this density region a theoretical treatment starting from finite nuclei is expected to be more reliable.

In the following we compare double folding potentials calculated from the microscopically derived interaction  $v(s, E, \rho)$  to empirical potentials obtained from model-unrestricted analyses of proton, alpha and  $^{16}\text{O}$  scattering from closed shell nuclei. These have been chosen in order to minimize coupled channel effects as well as the dominance of absorption phenomena in the scattering process. While proton scattering is sensitive to low densities  $\rho < \rho_0$ , the largest overlap densities up to  $3\rho_0$  occur in  $\alpha$ -scattering due to the large central density of the  $\alpha$ -particle. Heavy ion scattering on the other hand provides quite extended spatial regions of density overlap in the course of the scattering process coming thus closer to the dynamical realization of nuclear matter at high density.  $^{16}\text{O} + ^{16}\text{O}$  is the hitherto only heavy ion system where refractive nuclear rainbow scattering has been observed [4,5].

The energy dependence of the double folding potential originates from two different sources. One is the non-locality of the Fock-exchange terms, which yields a momentum-dependent local potential. The second source is the explicit energy dependence of the underlying effective NN interaction, see eq. (1). In order to emphasize the importance of this explicit energy dependence we compare in Fig. 2 the real part of the optical potential with the choice for the starting energy as discussed above (solid) with results obtained, when the off-shell or binding effects are ignored (dotted line,  $E = E_{\text{kin}}/A$ ,  $\langle S_{\text{P}} \rangle = \langle S_{\text{T}} \rangle = 0$ ). Ignoring Pauli effects this would correspond to an approach, which uses the T-matrix rather than the G-matrix for the effective NN interaction. One observes that this approach overestimates the real part by up to 20%. If the kinetic energy between projectile and target is ignored in the definition of the starting energy, the dashed line is obtained. This choice of the starting energy would be appropriate for calculating the binding energies of nuclei. We see that attempts which try to derive the nuclear equation of state from scattering experiments [5] without accounting for the explicit dependence of the interaction on the starting energy tend to overestimate the binding energy of nuclear matter as compared to more rigorous calculations.

Fig. 3 displays a comparison of our double folding potentials derived from the G-matrix to the empirical potentials extracted from scattering data by model-unrestricted analysis [2,4]. The hatched areas represent the uncertainties in the extracted potentials. We see that without adjustment of any parameter the calculations yield already a nearly quantitative description of the empirical potentials. Small readjustment of the potential strength ( $\lambda = 0.9 - 1.0$ ) leads to full agreement with the experimental results<sup>2</sup>, with the exception of the proton scattering

---

<sup>2</sup>We note that also the descriptions of the corresponding experimental angular distributions

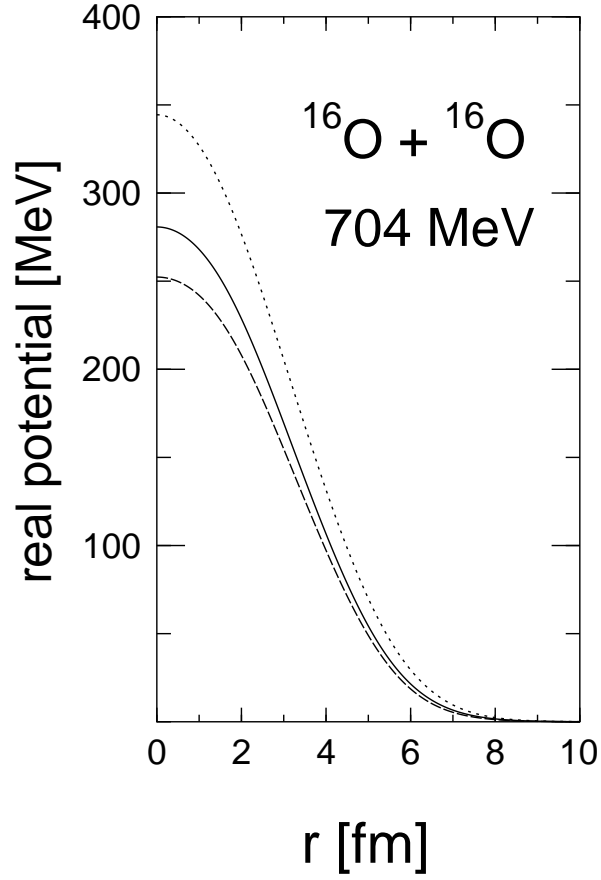


Figure 2: Double folding calculations for the real central scattering potential of  $^{16}\text{O} + ^{16}\text{O}$  at  $E = 704$  MeV. The solid curve shows the result by use of the correct choice of the starting energy, whereas for the other curves either the nucleon separation energies (dotted) or the kinetic energy between projectile and target (dashed) are neglected in the definition of the starting energy.

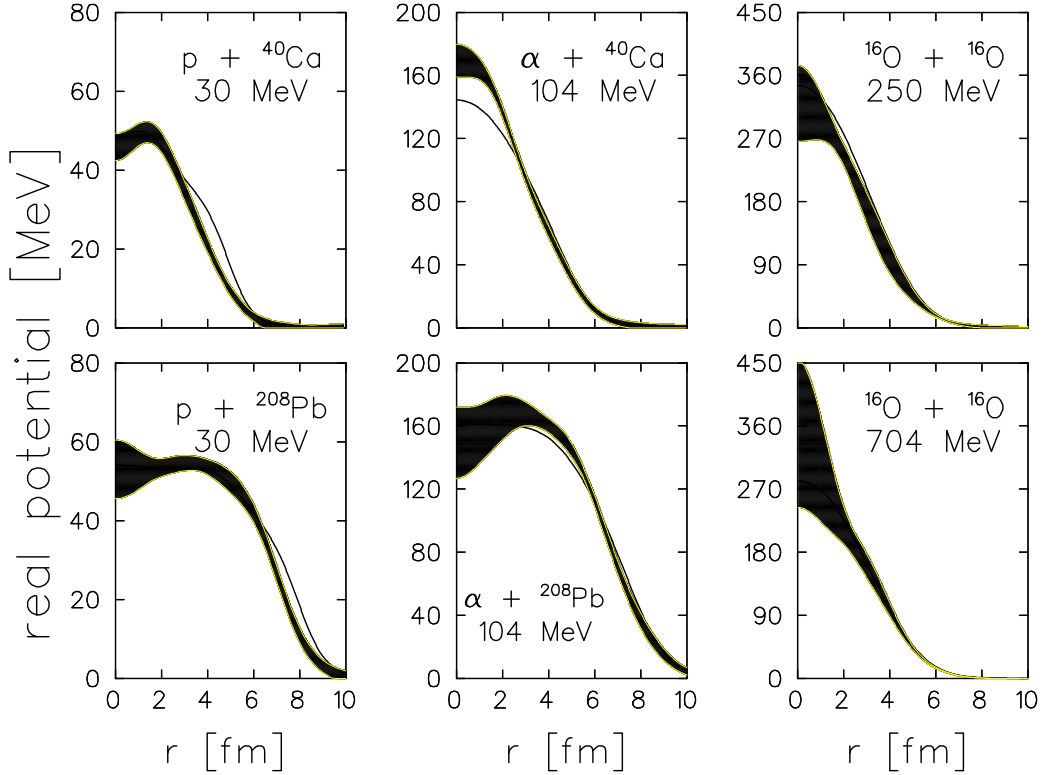


Figure 3: Fig. 3: Real central scattering potentials for the systems  $p + {}^{40}\text{Ca}$ ,  $p + {}^{208}\text{Pb}$ ,  $\alpha + {}^{40}\text{Ca}$ ,  $\alpha + {}^{208}\text{Pb}$  and  ${}^{16}\text{O} + {}^{16}\text{O}$  at  $E/A = 22 - 44$  MeV. The hatched areas represent the empirical potentials [2,4] with their uncertainties. The results of our double folding calculations are shown by the solid lines.

potentials. There the calculated potentials show a peculiar, bumpy behavior at the surface, which is not observed experimentally and which leads to a root mean square radius, which in case of  $p + {}^{40}\text{Ca}$  is larger by 30% than the experimental value and thus far beyond the experimental uncertainty. At a first glance this discrepancy is very surprising, since the conventional method of using a factorized effective interaction has led to a very satisfactory description of real central proton scattering potentials [2]. The failure of our more rigorous calculation can be traced back to the very different density dependence of “ $\sigma$ ” and “ $\omega$ ” exchange in the effective interaction at low densities, as is apparent from fig. 1. Since in the conventional calculations with factorized interactions implicitly identical density dependencies are assumed for “ $\sigma$ ” and “ $\omega$ ” exchange, this problem has not been encountered there. On the other hand the failure of the nuclear matter calculations for  $\rho < \rho_0$  is not totally unexpected as we discussed above.

In summary we have exploited the strong sensitivity of the real nucleus-nucleus scattering potentials to the density dependence of the underlying effective interactions. Our results are comparable to those obtained in the model-unrestricted analyses.

NN-interaction to test a new theoretical derivation of the latter, starting from nuclear matter calculations. This inherently energy- and density-dependent interaction  $v(s, E, \rho)$  reproduces empirical heavy and light ion scattering potentials (real part) on a quantitative level, with the exception of proton scattering. The failure there can be traced back to the problems of parametrizing a  $G$ -matrix for nuclear matter at densities  $\rho < \rho_0$ . At high densities,  $\rho > \rho_0$ , the good agreement with the results from scattering data confirms the weak density dependence of  $v(s, E, \rho)$  which leads [4,9,10] to a soft equation of state for nuclear matter with a compressibility of  $K \approx 190$  MeV. We note, however, that the nuclear matter saturation properties calculated with  $v(s, E, \rho)$ ,  $E/A = -13$  MeV and  $\rho_0 = 0.22$  fm $^{-3}$ , are slightly off the empirical values ( $-16$  MeV,  $0.17$  fm $^{-3}$ ) in resemblance of the well-known Coester-band problem [9].

## References

- [1] C.J. Batty, E. Friedman, H.J. Gils and H. Rebel, *Adv. in Nucl. Phys.* **19** (1989) 1 and references therein
- [2] M. Ermer et al., *Phys. Lett.* **B224** (1989) 40
- [3] N. Heberle et al., *Phys. Lett.* **B250** (1990) 15
- [4] G. Bartnitzky et al., *Phys. Lett.* **B365** (1996) 23  
G. Bartnitzky, Ph.D. thesis, University of Tübingen, 1995
- [5] D.T. Khoa et al., *Phys. Rev. Lett.* **74** (1995) 34
- [6] J. Siegler, Diploma thesis, University of Tübingen, 1995
- [7] N. Anantaraman, H. Toki and G.F. Bertsch, *Nucl. Phys.* **A398** (1983) 269;  
G.F. Bertsch et al., *Nucl. Phys.* **A284** (1977) 399
- [8] D.T. Khoa and W. von Oertzen, *Phys. Lett.* **B342** (1995) 6
- [9] R. Machleidt *Adv in Nucl. Phys.* **19** (1989) 189
- [10] P. Czerski, H. Müther and W. Dickhoff, *J. Phys.* **G20** (1994) 425